Journal of Integrative Neuroscience

J. Integr. Neurosci. **2026**; 25(7): 50932
https://doi.org/10.31083/JIN50932

Original Research

Extracellular Vesicle-Mediated Delivery of VEGF and NGF Protects Dopaminergic Neurons in 6-OHDA-Induced Parkinson's Disease Models

Wenyu Yan[1], Xianyue Meng[2], Yan Wang[3,4], Chuanfei Wei[5], Fabin Han[5,*], Xueli Li[2,*]

[1]Department of Neurology, Shandong First Medical University, 250117 Jinan, Shandong, China
[2]Department of Neurology, Liaocheng Hospital Affiliated to Shandong First Medical University (Liaocheng People's Hospital), 252000 Liaocheng, Shandong, China
[3]Department of Precision Key Laboratory, Liaocheng People's Hospital, Liaocheng Hospital Affiliated to Shandong First Medical University, 252000 Liaocheng, Shandong, China
[4]Department of Biomedical Engineering, College of Life Science and Technology, Huazhong University of Science and Technology, 430074 Wuhan, Hubei, China
[5]Key laboratory for Stem cell & Regenerative Medicine translation of Health Commission of Shandong Province, Liaocheng Hospital Affiliated to Shandong First Medical University (Liaocheng People's Hospital), 252000 Liaocheng, Shandong, China
*Correspondence: fhan2013@126.com (Fabin Han); lixueli2001@163.com (Xueli Li)
Academic Editor: Gernot Riedel
Submitted: 11 February 2026 Revised: 28 April 2026 Accepted: 6 May 2026 Published: 27 July 2026

Abstract

Background: Parkinson's disease (PD) is a neurodegenerative disorder marked by motor dysfunction. No definitive methods exist to repair damaged neurons. Vascular endothelial growth factor (VEGF) and nerve growth factor (NGF) are two neuroprotective agents that work synergistically. However, these large molecular proteins have difficulty crossing the blood–brain barrier (BBB). Extracellular vesicles (EVs) offer superior targeting and low immunogenicity, making them excellent carriers. In this study we examined the protective effects of VEGF and NGF in a cell model and evaluated the therapeutic potential of VEGF–NGF contained within EVs in PD rats. **Methods:** EVs were isolated using sequential differential centrifugation and characterized using transmission electron microscopy, nanoparticle tracking analysis, and western blotting (WB). VEGF and NGF were loaded into the EVs using a saponin-assisted method to create VEGF@EVs, NGF@EVs, and VEGF/NGF@EVs. The viability of 6-hydroxydopamine hydrochloride (6-OHDA)-induced SH-SY5Y cells was measured using the cell counting kit-8 assay before and after treatment with VEGF and NGF. Autophagy levels were assessed using WB, and the role of autophagy was further explored using the autophagy inhibitor chloroquine. Unilateral PD rat models were established via stereotactic injection of 6-OHDA into male Sprague–Dawley rats. Behavioral changes were monitored before and after treatment. Neuronal recovery, neurotransmitter levels, and autophagy levels in the rat brains were evaluated using immunohistochemistry, enzyme-linked immunosorbent assay, and WB. **Results:** VEGF/NGF@EVs significantly enhanced the viability of 6-OHDA-induced SH-SY5Y cells. A complete autophagic process was identified as essential for this protective effect. The intranasal administration of VEGF/NGF@EVs improved motor behavior in PD rats, with performance better than that of single growth factor treatments. The number of tyrosine hydroxylase (TH)–positive neurons, TH protein expression, and dopamine content were significantly increased. In addition, the level of autophagy in the rat substantia nigra was elevated. **Conclusions:** VEGF/NGF@EVs exert protective effects in both *in vitro* and *in vivo* 6-OHDA-induced PD models by promoting autophagy, demonstrating greater efficacy than either growth factor alone. By transplanting VEGF/NGF@EVs into PD rats, we showed that these vesicles can effectively cross the BBB and deliver targeted therapy to the central nervous system. This study highlights the significant potential of EV-mediated protein transplantation strategies for treating neurological disorders.

Keywords: Parkinson's disease; vascular endothelial growth factor; nerve growth factor; extracellular vesicles; autophagy

1. Introduction

Parkinson's disease (PD) is the second most common neurodegenerative disorder. Its main pathological features include the progressive loss of dopaminergic neurons and the formation of Lewy bodies within remaining neurons [1]. The notable decrease in neurotransmitter levels resulting from damage to dopaminergic neurons is a major factor in the characteristic motor dysfunction of PD [2]. Currently, dopamine (DA) replacement therapy remains the main treatment for PD. However, long-term use of these medications can cause side effects, and their capacity to repair neuronal damage is limited [3].

Autophagy helps remove damaged organelles and misfolded proteins, playing a vital role in maintaining homeostasis [4]. Autophagy dysfunction is considered a key contributor to the pathological microenvironment and the buildup of abnormal proteins, such as α-synuclein, which is linked to neuronal damage [5,6]. Recent studies have shown that curcumin, exosomes, and DA-conjugated

extracellular vesicles (EVs) can exert protective effects in PD models by enhancing autophagy [7,8,9].

Deficiencies in neurotrophic factors are another important pathological feature associated with PD. Vascular endothelial growth factor (VEGF) improves the pathological microenvironment and exerts direct protective and pro-survival effects on dopaminergic neurons [10,11]. Our previous study has confirmed the protective effect of VEGF gene transplantation on dopaminergic neurons [12]. Furthermore, VEGF participates in autophagy regulation [13]. Nerve growth factor (NGF) supports the growth, function, and repair of the nervous system, playing a key role in neuronal survival, growth, axonal guidance, and synaptic plasticity [14,15,16]. An early study reported a significant decline in serum NGF levels in patients with PD and rat models [17]. Another study documented that NGF inhibits 1-methyl-4-phenyl-1,2,3,6-tetrahydropyridine (MPTP)–induced apoptosis in PC12 cells [18]. These findings imply that NGF supplementation may be a promising strategy for neuronal protection in PD. Additionally, NGF can contribute to angiogenesis by stimulating VEGF production [19]. Studies have confirmed that VEGF and NGF exert a synergistic effect on regenerating vascular and neural tissues. However, limited literature is available on their application in the central nervous system [20,21]. Based on these findings, this study hypothesized that coregulating VEGF and NGF could offer new therapeutic strategies for PD. Nonetheless, their large molecular protein nature makes it difficult for them to cross the blood–brain barrier (BBB). Therefore, finding a safe and effective delivery method is a critical challenge in current research.

EVs are membrane-bound nanoparticles with a bilayer structure. According to their diameter, they are categorized into two types: small EVs (<200 nm) and large EVs (>200 nm) [22]. The ability of EVs to cross the BBB makes them an excellent drug delivery system. Multiple studies have shown that EV-based delivery systems can effectively cross the BBB, enable targeted drug delivery, and improve the condition of patients with PD [23,24,25].

Therefore, this study examined the protective effects of combining VEGF and NGF in PD models and confirmed their influence on autophagy levels. Moreover, an *in vivo* delivery system was developed using EVs as carriers to investigate the neuroprotective effects of these nanoparticles on PD rats. This research helped assess the potential of the EV–protein delivery system for treating PD, offering new insights and approaches for clinical therapy.

2. Materials and Methods

2.1 Cell Culture and Characterization

Human umbilical cord mesenchymal stem cells (HUC-MSCs; preserved in Laboratory for Stem Cell and Regenerative Medicine, Liaocheng, China) were cultured in DMEM/F12 medium (D6421, Sigma-Aldrich, Taufkirchen, Germany) supplemented with 10% fetal bovine serum (FBS; F0193, Sigma-Aldrich), 1% Minimum Essential Medium non-essential amino acids (MEM NEAA ;11140050, Gibco, USA), 1% penicillin-streptomycin (Pen Strep; 15070063, Gibco, USA), and 1% L-glutamine (25030081, Gibco, USA) under 37 °C in a humidified incubator (3111, Thermo Fisher Scientific, Waltham, MA, USA) with 5% CO_2 atmosphere.

HUC-MSCs were digested and counted, and then resuspended in 200 µL of sterile PBS to prepare a homogeneous single-cell suspension (1×10^6 cells/mL). Appropriate aliquots of the cell suspension were incubated with the following antibodies for 30 min in the dark: anti-cluster of differentiation (CD)73-phycoerythrin (PE) (1:40, 550257, BD Biosciences, San Jose, CA, USA), anti-CD90-fluorescein isothiocyanate (FITC; 1:40, 561969, BD Biosciences), anti-CD34-PE (1:40, 348057, BD Biosciences), and anti-CD14-peridinin–chlorophyll protein (PerCP; 1:40, 340660, BD Biosciences). Then, the cells were washed three times with 2 mL of PBS (300 ×*g*, 5 min each), resuspended in 500 µL of staining buffer and subjected to flow cytometry. The following controls were included: (1) unstained cells to determine autofluorescence and set the forward/side scatter gate; (2) isotype-matched antibodies for each fluorochrome. The flow cytometry gating strategy was performed as follows: cells were first gated on the main population using forward scatter area (FSC-A) versus side scatter area (SSC-A) to exclude debris and dead cells. Single cells were then selected by gating on FSC-A versus forward scatter height (FSC-H) to exclude doublets. Subsequently, the expression of surface markers was analyzed on the singlet gate. Data were analyzed using FlowJo (10.8.1, BD Biosciences).

SH-SY5Y cells (Procell Life Science & Technology Co., Ltd., Wuhan, China) were cultured in DMEM/F12 medium containing 10% FBS and 1% Pen Strep under the conditions of 37 °C in a humidified incubator with 5% CO_2.

HUC-MSCs and SH-SY5Y cells were validated for their identity by surface marker analysis using flow cytometry or STR and tested negative for mycoplasma.

2.2 EVs Separation and Characterization

After HUC-MSCs reached 80–90% confluence, the original medium was removed, and the cells were washed twice with sterile PBS to remove residual serum. The cells were then cultured in FBS-free medium for 48 h. The cell supernatant was collected and subjected to sequential differential centrifugation at 4 °C as follows: 300 ×*g* for 10 min (to remove live cells), 2000 ×*g* for 10 min (to remove dead cells), and 10,000 ×*g* for 30 min (to remove debris and organelles). After each centrifugation step, the supernatant was carefully transferred into a new tube. The clarified supernatant was then filtered through a 0.22-µm membrane, transferred into a polycarbonate tube, and centrifuged at 100,000 ×*g* for 70 min. The supernatant was discarded, and the pellet was resuspended in sterile PBS, followed by an-

other centrifugation at 100,000 ×*g* for 70 min. The final pellet was resuspended and stored at −80 °C.

The ultrastructure and size distribution were characterized via transmission electron microscope (TEM, TECNAI G2 12, FEI, Hillsboro, OR, USA) and nanoparticle tracking analysis (NTA, ZetaView PMX-120, Particle Metrix, Meerbusch, Germany). Concentration was determined by the bicinchoninic acid (BCA) protein method (P0012S, Beyotime, Shanghai, China). Protein marker expression was assessed by western blotting (WB), with antibodies against CD9 (1:1000, Ab263019, Abcam, Cambridge, UK), CD63 (1:1000, Ab134045, Abcam), tumor susceptibility gene 101 (TSG101; 1:1000, Ab125011, Abcam), and heat shock protein 70 (HSP70; Ab181606, 1:1000, Abcam).

2.3 Loading VEGF and NGF Into EVs

VEGF (RPA143Hu01, Cloud-Clone Corp., Wuhan, China) and NGF (RPA105Hu01, Cloud-Clone Corp.,) were loaded into EVs using saponin (S299339, Aladdin, Shanghai, China) to prepare VEGF@EVs, NGF@EVs, and VEGF/NGF@EVs. The protocol was as follows. First, a reaction mixture (final volume of 200 µL) consisting of protein, purified EVs (1 mg/mL), saponin (0.2%), and sterile 1× PBS was incubated on a shaker at room temperature (RT) for 30 min. Specifically, VEGF@EVs contained 10 µg VEGF, NGF@EVs contained 20 µg NGF, and VEGF/NGF@EVs contained both 10 µg VEGF and 20 µg NGF. Subsequently, the sample was transferred to the Ultrafiltration Spin Columns (FUF510, Beyotime) and centrifuged for 10 min at 4000 ×*g*. The retained samples were collected.

2.4 ELISA Assay for VEGF and NGF Protein Levels

A mixed solution containing equal volumes of radioimmunoprecipitation assay (RIPA) buffer (P0013B, Beyotime) and EVs particles (prepared in the previous step) was incubated on an ice bath for 30 min. The concentration of VEGF and NGF was analyzed by using the enzyme-linked immunosorbent assay (ELISA) kit (E-EL-H0111, E-EL-H1205, Elabscience, Wuhan, China).

Samples and reference standards were added to each well. Then, the biotinylated antibody was supplemented immediately and incubated for 45 min at 37 °C. The plates were washed with buffer. Horseradish peroxidase (HRP)-conjugate fluid was supplemented and incubated for 30 min at 37 °C. After washing, the substrate solution was supplemented and incubated for 15 min, after which the stop solution was added. The optical density was immediately recorded at 450 nm by using a plate reader (1681130, Bio-Rad, Hercules, CA, USA).

2.5 Internalization of EVs and VEGF/NGF in SH-SY5Y Cells

To evaluate EV internalization, EVs were labeled with PKH26 and incubated with SH-SY5Y cells for 4 h. After which, the cells were washed with PBS and observed by fluorescence microscopy (Nikon, Tokyo, Japan).

VEGF and NGF were labeled with Alexa Fluor™ 488 (AF488, P1253S, Beyotime), and the labeled proteins were loaded into EVs. Following co-incubation with SH-SY5Y cells for 4 h, the cells were washed and examined by fluorescence microscopy.

2.6 Cell Viability Assay

Cell viability was assessed by cell counting kit-8 (CCK-8) assay (C0037, Beyotime). SH-SY5Y cells were seeded into 96-well plates at 1×10^5 cells/well density and cultured overnight, followed by exposure to varying concentrations of 6-hydroxydopamine hydrochloride (6-OHDA, H4381, Sigma-Aldrich) for 12, 18, and 24 h.

To assess the beneficial effects of VEGF and NGF, SH-SY5Y cells were exposed to 6-OHDA (50 µM) and co-cultured with VEGF and NGF at concentrations of 10, 25, 50, and 100 ng/mL for 12 h. The control group consisted of cells that were normally cultured. And a blank control without cells was established to correct for any background absorbance.

Then, the cells were incubated with 10 µL of CCK-8 reagent for 2 h, and the optical density at 450 nm was recorded using a microplate reader. OD_{Exp}, OD_{Con} and OD_0 represent the optical density of the experimental group, control group and blank control, respectively. Cell viability was calculated using the following formula:

$$\text{Cell viability } (\%) = \frac{ODExp - OD0}{ODCon - OD0} \times 100\%$$

2.7 Animals

A total of 58 adult male SD rats (200–220 g; Nanjing Huimiaoxin Biotechnology Co., Ltd., Nanjing, China) were used in this study. The rats were housed under specific-pathogen-free conditions (humidity 40–60%, temperature 22 ± 2 °C, 12-h dark/light cycle) and allowed free access to food and water.

2.8 Biodistribution of EVs

For *in vivo*-distribution analysis, EVs were labeled by PKH26 (Beyotime; 551-nm excitation, 567-nm emission) and administered intranasally to each rat at a dose of 20 µg (in 20-µL PKH26 dye solution). An identical volume of normal saline was administered to the control group. At 4 h and 16 h post-administration, the rats were deeply anesthetized with 5% isoflurane. Under deep anesthesia, rats were transcardially perfused with 4% paraformaldehyde (PFA, 158127, Sigma-Aldrich), which served simul-

taneously as a terminal fixation procedure and the means of euthanasia. Following perfusion, organs were harvested for imaging analysis by the Small Animal *Ex Vivo* Imaging System (IVIS Lumina III, PerkinElmer, Waltham, MA, USA).

2.9 Rats Model and Grouping

An animal model of PD was established in adult male SD rats via a stereotaxic injection of 6-OHDA (H4381, Sigma-Aldrich). Isoflurane (R510-22-10, RWD, Shenzhen, China) was administered via a facemask at an induction concentration of 2%–4% and a maintenance concentration of 1.0%–2.5%. After anesthetizing with isoflurane, the rats were placed in a stereotaxic apparatus (RWD, Shenzhen, China). A total of 10 µg of 6-OHDA was dissolved in 10 µL of saline containing 0.1% ascorbic acid (1.00468, Sigma-Aldrich), which was injected into two sites at the following coordinates: AP –4.8 mm, ML –1.9 mm, DV –7.5 mm, and AP –4.8 mm, ML –1.1 mm, and DV –8.0 mm. The blank group received the same dose of saline. To prevent reflux, the needle was maintained in the same position for 5 min following injection. Postoperatively, the rats were housed individually.

Apomorphine (APO, PHR2621, Sigma-Aldrich)-induced rotation was used to assess behavioral changes on days 7, 14 and 21 after modeling. Postoperatively, the rats were administered APO (0.5 mg/kg) via intramuscular injection in the neck. Following a 5-min acclimation period, the rotational behavior was monitored continuously for 30 min. Animals exhibiting more than 210 rotations in 30 min were classified as successful models.

The successful models were randomly assigned into the following five groups (n = 8): 6-OHDA, EVs, VEGF@EVs, NGF@EVs, and VEGF/NGF@EVs. Intranasal administration was performed using a small pipette. Each rat received 10 µL of the solution per nostril at 2-min intervals, once daily for two consecutive weeks. Behavior changes were checked at 7 days and 14 days. All animals were anaesthetised and transcardially perfused with saline followed by 4% paraformaldehyde (PFA) immediately after the final behavioural test.

2.10 Immunohistochemistry

After induction of anesthesia with 3–4% isoflurane, the rats were placed supine on a flat plate with limbs immobilized. A transverse incision was created at the xiphoid process to expose the diaphragm and thoracic cavity, revealing the heart. A perfusion needle was inserted into the cardiac apex and secured with hemostatic forceps. Ophthalmic scissors were carefully used to make a transverse incision at the right atrial appendage to access the venous blood. Initial perfusion was performed with normal saline. After confirming that there was no fresh blood flow from the atrial appendage, direct sampling or sampling after fixation was performed via injection with 4% PFA (158127, Sigma-Aldrich).

After fixation by immersion in 4% PFA, the rat brains were dehydrated, cleared, and embedded in molten paraffin. The embedded tissues were sectioned with a microtome (RM2235, Leica, Wetzlar, Germany), and the sections were dried at 65 °C for 2 h.

Immunohistochemical staining was performed as follows. After antigen retrieval using the trypsin (X1020, Solarbio, Beijing, China) digestion solution, endogenous peroxidases were quenched with 3% H_2O_2. The sections were blocked and then incubated with tyrosine hydroxylase (TH)-specific primary antibody (1:500, ab137869, Abcam) overnight at 4 °C. Then the sections were incubated with biotinylated secondary antibody (1:100; SP0021, Solarbio) at 37 °C for 30 min, followed by incubation with streptavidin-peroxidase conjugate (1:100; SP0021, Solarbio) at 37 °C away from light for 30 min. Staining was performed using 3,3′-diaminobenzidine (DAB; SP0021, Solarbio) substrate for 5 min, followed by washing with double-distilled water (ddH_2O) for 7 min. Counterstaining was performed with hematoxylin (C0107, Beyotime) for 1 min, followed by dehydration and mounting with neutral balsam (C0173, Beyotime). Images were acquired using a light microscope (Nikon).

2.11 ELISA Assay for DA

The striatum was dissected from the entire brain. After weighing, the tissue was immediately placed in liquid nitrogen for 5 min and stored at –80 °C. The tissue samples were transferred into pre-cooled PBS containing protease inhibitors (ST506, Beyotime). The tissue was homogenized using a homogenizer (SWE-FP PLUS, Servicebio, Wuhan, China). The homogenate was centrifuged for 15 min at 15,000 ×*g* at 4 °C. The supernatant was collected, aliquoted, and stored at -80 °C. The concentration of DA was detected by using an ELISA kit (E-EL-0046, Elabscience).

2.12 Western Blotting Analysis

For the analysis of the protein of interest from SH-SY5Y cells, the protein extracts were prepared using RIPA containing 1× phenylmethylsulfonyl fluoride (PMSF, ST506, Beyotime). After 20 min of incubation on an ice bath, the cell lysate was collected and centrifuged for 15 min at 15,000 ×*g* at 4 °C. The supernatants were obtained and aliquoted.

For the tissue samples, the midbrain was homogenized in the same solution for 15 min. The homogenate was centrifuged for 15 min at 15,000 ×*g* at 4 °C. The supernatants were obtained and aliquoted. The protein concentrations were measured by BCA.

The protein samples were mixed with 5× loading buffer (P0015, Beyotime) at a 4:1 ratio and heated at 100 °C for 10 min. Separation and stacking gels were prepared based on the molecular weight of the target protein.

After solidification, the denatured samples were loaded and electrophorized. Following electrophoresis, gel slices corresponding to the target molecular weight were excised, and the proteins were transferred onto polyvinylidene fluoride (PVDF) membranes (IPVH00010, Merck Millipore, Billerica, MA, USA). The membranes were blocked in 5% non-fat milk for 1 h at RT and then incubated overnight at 4 °C with primary antibodies against anti-microtubule-associated protein 1 light chain 3 beta (LC3B; ab192890, 1:1000, Abcam, Cambridge, MA, USA), anti-sequestosome 1 (p62; AG4400, 1:1000, Beyotime, Shanghai, China), anti-tyrosine hydroxylase (TH; ab137869, 1:1000, Abcam), and anti-β-actin (AF5003, 1:1000, Beyotime). After washing with Tris-buffered saline with Tween 20 (TBST, ST673, Beyotime), the membranes were incubated with HRP-conjugated anti-rabbit antibodies (1:1000, A0208, Beyotime) for 2 h with shaking. The protein bands were visualized using enhanced chemiluminescence (ECL) solution (P0018S, Beyotime), and densitometric analysis was performed using ImageJ (version 1.54g, National Institutes of Health, NIH, USA).

2.13 Statistical Analysis

All experimental data were represented as the mean ± standard deviation (SD). Each independent experiment was repeated at least three times (n ≥3 biologically independent samples per group). One-way analysis of variance (ANOVA) and two-way ANOVA followed by Tukey's post-hoc test were conducted using GraphPad Prism 10 (GraphPad, San Diego, CA, USA). $p < 0.05$ was considered to indicate statistical significance.

3. Results

3.1 Characterization of HUC-MSCs

Flow cytometry analysis revealed that the cells strongly expressed the mesenchymal stem cell markers CD73 and CD90, with positivity rates >95%, while exhibiting minimal expression of the hematopoietic markers CD14 and CD34. These phenotypic features align with those of HUC-MSCs (Fig. 1A).

3.2 Identification of EVs

EVs were isolated from cultured media. TEM observations revealed that the extracted EVs had a cup-shaped membrane structure (Fig. 1B). WB showed that EVs expressed CD63, CD9, TSG101, and HSP70, which are EVs marker proteins (Fig. 1C). NTA determined the concentration and size distribution of the particles. The average diameter of the EVs was 73 nm (Fig. 1D), increasing to 82 nm after saponin treatment (Fig. 1E). Saponin permeabilization treatment increased the EVs diameter (Fig. 1F), suggesting that some vesicles may undergo fusion, but the overall size variation was minimal. Based on these findings, the extracted particulate matter can be identified as EVs, making them suitable for subsequent experimental studies.

3.3 Encapsulation Efficiencies and Drug Loading Rates of VEGF and NGF in EVs

The drug loading rates of VEGF in VEGF@EVs and VEGF/NGF@EVs were 8.689% ± 1.602% and 5.532% ± 1.144%, respectively. Similarly, the loading rates of NGF in NGF@EVs and VEGF/NGF@EVs were 14.293% ± 2.787% and 5.804% ± 1.267%, respectively (Table 1). After mixing, the drug-loading rates of VEGF and NGF decreased, but the reduction was more pronounced for NGF, likely due to its larger molecular weight.

3.4 Internalization of EVs and VEGF/NGF by SH-SY5Y Cells

The red fluorescence in Fig. 2 shows the internalization of EVs. The figures demonstrate that EVs can be internalized by SH-SY5Y cells and are evenly distributed around the nucleus. The green fluorescence in Fig. 2 displays the distribution of AF488-labeled VEGF/NGF in SH-SY5Y cells. The results indicate that the proteins can be internalized by cells via EVs.

3.5 Enhancement of the Viability of SH-SY5Y Cells by VEGF/NGF@EVs

SH-SY5Y cells were treated with various concentrations of 6-OHDA for 12 h. CCK-8 analysis indicated that 6-OHDA reduced cell viability in a concentration-dependent manner (Fig. 3A). Exposure to 50 μM 6-OHDA for 12 h decreased SH-SY5Y cell viability to 50% of the control level ($p < 0.001$).

To investigate the effects of VEGF and NGF, their optimal concentrations were examined (Fig. 3B). Four concentrations were tested: 10 ng/mL, 25 ng/mL, 50 ng/mL, and 100 ng/mL. Cell viability was significantly improved when the growth factor concentration was 50 ng/mL ($p < 0.05$). The results for the other concentrations are shown in the **Supplementary Material**. Statistical analysis showed that cell viability in the VEGF/NGF@EVs group was significantly higher than that in the VEGF@EVs and NGF@EVs groups, suggesting that the combined use of VEGF and NGF is more effective than either growth factor alone. The protective effect of VEGF/NGF@EVs against 6-OHDA-induced SHSY5Y cell injury was notably decreased when autophagy was blocked using chloroquine (CQ), suggesting that autophagy plays a key role in the neuroprotective effect of VEGF/NGF@EVs.

Moreover, pure EVs did not exert protective effects on 6-OHDA-induced SH-SY5Y cells, excluding potential confounding effects from the carrier. Furthermore, treatment of normal SH-SY5Y cells with VEGF and NGF alone did not affect their viability, implying that these concentrations are nontoxic to healthy cells (Fig. 3C).

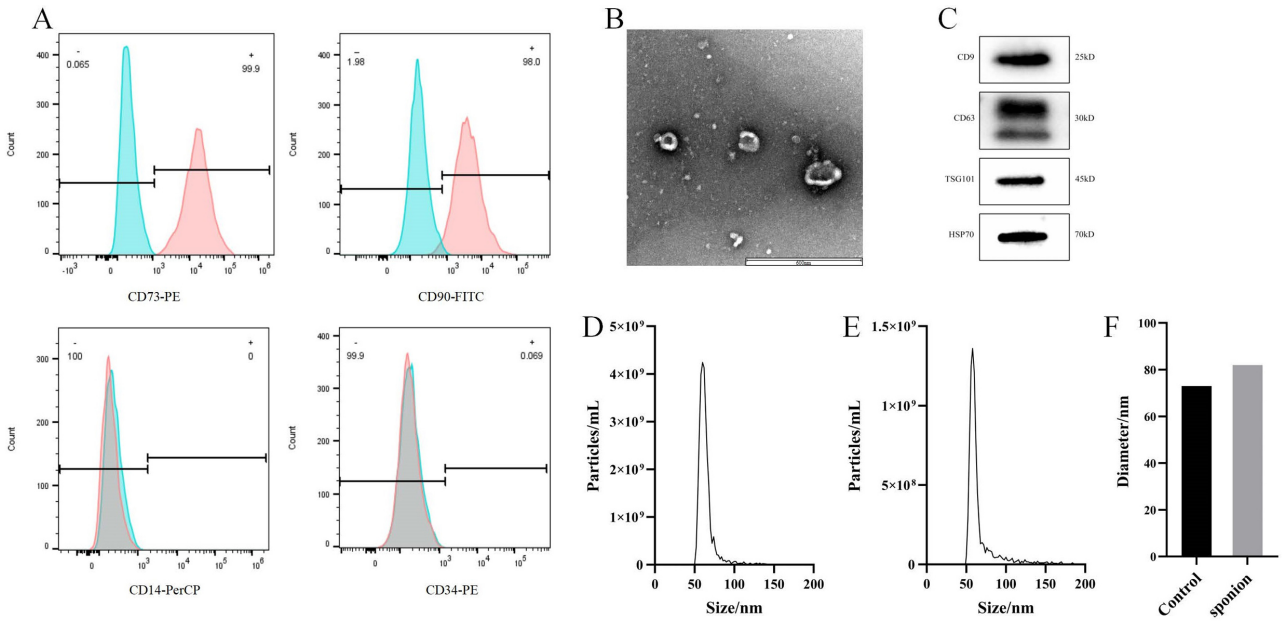

Fig. 1. Characterization of HUC-MSCs and EVs. (A) Flow cytometric assay of the surface marker of HUC-MSCs. (B) Morphological characteristics of EVs observed under TEM. Scale bar: 600 nm. (C) Western blotting analysis of CD9, CD63, TSG101, and HSP70 expressions. (D) Particle size distribution of EVs. (E) Particle size distribution of EVs after saponin treatment. (F) Comparison of particle diameters before and after saponin treatments. HUC-MSCs, human umbilical cord mesenchymal stem cells; EVs, extracellular vesicles; TEM, transmission electron microscope; CD9, Cluster of Differentiation 9; CD63, Cluster of Differentiation 63; TSG101, Tumor Susceptibility Gene 101; HSP70, Heat Shock Protein 70; PE, Phycoerythrin; FITC, Fluorescein Isothiocyanate.

Table 1. EE and DL of VEGF and NGF in different nanoparticles (%).

Formulation	EE of VEGF	DL of VEGF	EE of NGF	DL of NGF
VEGF@EVs	19.085 ± 3.892	8.689 ± 1.602	-	-
NGF@EVs	-	-	16.776 ± 3.663	14.293 ± 2.787
VEGF/NGF@EVs	11.737 ± 2.585	5.532 ± 1.144	6.178 ± 1.437	5.804 ± 1.267

EE, encapsulation efficiency; DL, drug loading rate; VEGF, vascular endothelial growth factor; NGF, nerve growth factor.

3.6 The Ability of VEGF/NGF@EVs to Increase the Autophagy of 6-OHDA-Induced SH-SY5Y Cells

LC3B and p62 (SQSTM1) are important markers of autophagy. LC3B, a main part of the autophagosome membrane, directly indicates autophagic activity. Its levels correlate positively with autophagy. p62, a selective autophagy adaptor, detects ubiquitinated cargos and binds to LC3B-II to help with autophagic degradation. p62 levels are inversely related to autophagic activity. Its buildup signals defective autophagic flux, making it a dependable marker of autophagic degradation efficiency.

To determine whether VEGF/NGF@EVs induce autophagy, LC3B and p62 expressions were examined using WB (Fig. 4A). Compared with the control group, the LC3B-II/I ratio and p62 levels increased in 6-OHDA-induced SH-SY5Y cells, indicating autophagy initiation but impaired degradation. Treatment with VEGF/NGF@EVs further increased the LC3B-II/I ratio ($p < 0.05$) and significantly decreased p62 expression (Fig. 4B,C), suggesting enhanced autophagosome formation and restored autophagic degradation, thereby reestablishing a complete autophagic cycle.

To confirm the role of autophagy, CQ, a late-stage autophagy inhibitor, was used. CQ treatment further increased the LC3B-II/I ratio and led to p62 accumulation, confirming blockade of autophagic flux. Under these conditions, cell viability was significantly reduced, and the protective effect of VEGF/NGF@EVs was mostly lost. These findings suggest that autophagy is a key mechanism by which VEGF/NGF@EVs exert their protective effects.

3.7 The Ability of VEGF/NGF@EVs to Cross the BBB and Relieve the Asymmetric Rotation Defect in PD Rats

Biodistribution analysis showed that four hours after nasal administration, PKH26-labeled EVs were detected in the brain (Fig. 5A). Furthermore, EVs delivered via nasal spray preferentially reached the brain (Fig. 5B).

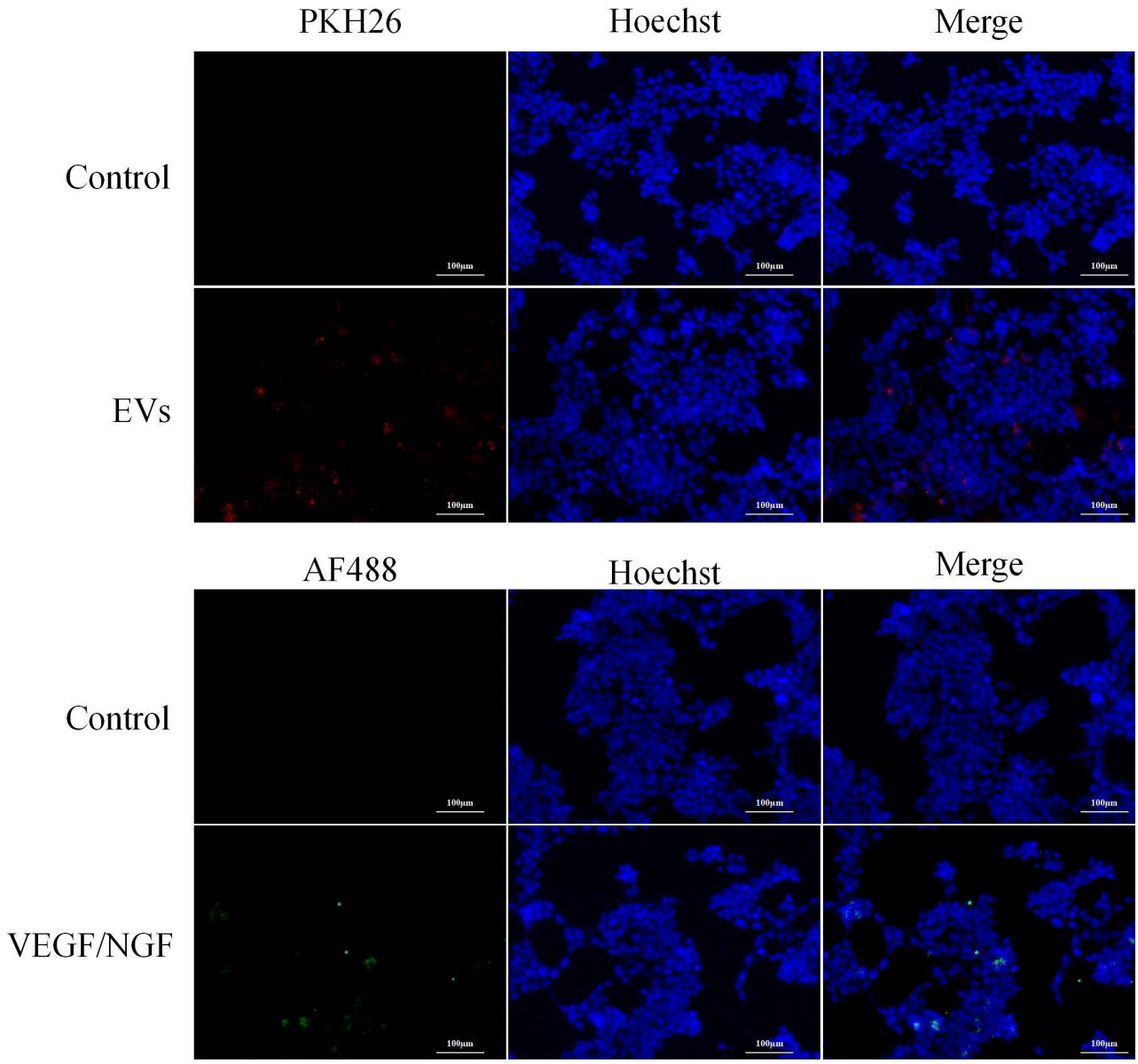

Fig. 2. Internalization of EVs and VEGF/NGF in SH-SY5Y cells by fluorescence microscopy. Scale bar: 100 μm. AF488, Alexa Fluor® 488; PKH26, PKH26 Red Fluorescent Cell Linker.

PD rat models were treated according to the previous groups. The APO-induced rotation was assessed on days 7 and 14 after administration. After 7 days of treatment, all groups except for the EVs group showed a significant reduction in rotation frequency, including the VEGF@EVs group, NGF@EVs group, and VEGF/NGF@EVs group, indicating that the drug intervention had produced preliminary therapeutic effects (Fig. 5C). After 14 days of treatment, the number of rotations in all treatment groups decreased further compared with the 7-day mark (Fig. 5D). The VEGF/NGF@EVs group demonstrated a significantly greater reduction in rotation frequency compared with the single-factor groups and showed more improvement than at the 7-day point (Fig. 5E). These differences were statistically significant, suggesting that the combined VEGF/NGF@EVs intervention more effectively mitigates motor dysfunction in PD rats.

3.8 The Ability of VEGF/NGF@EVs to Significantly Reduce Substantia Nigra(SN) Dopaminergic Neuron Loss and Upregulate the Levels of DA in the Striatum of PD Rats

Immunohistochemical staining was performed to specifically detect TH protein(Fig. 6A), and the survival status of dopaminergic neurons was assessed (Fig. 6C). The results indicated that compared with the contralateral side, the number of neurons in the damaged substantia nigra after 6-OHDA modeling was significantly reduced,

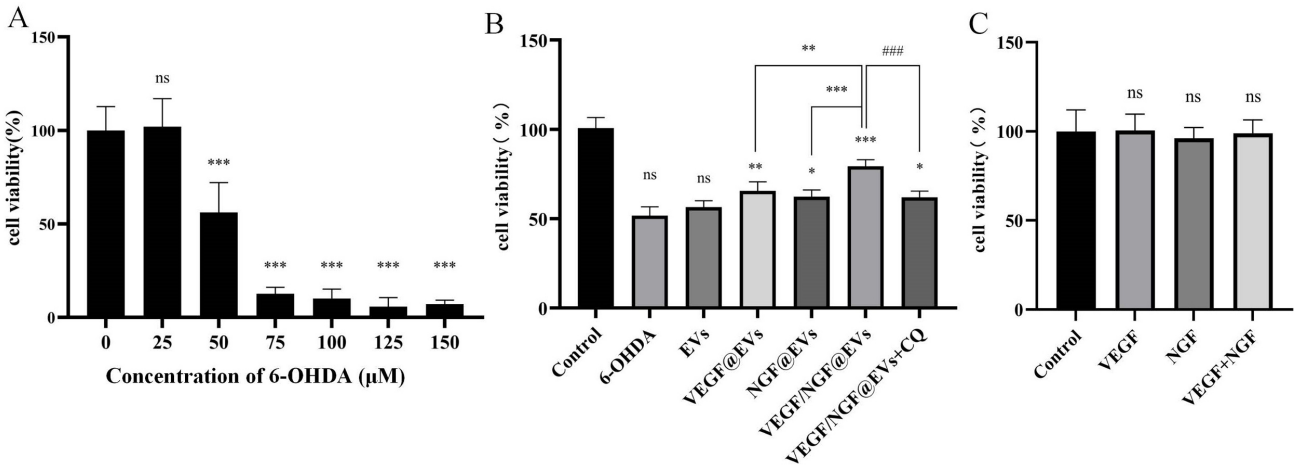

Fig. 3. Cell viability of SH-SY5Y. (A) Cell viability of SH-SY5Y cells induced by different concentrations of 6-OHDA (n = 6). (B) Effects of 50 ng/mL growth factors on the viability of 6-OHDA-induced SH-SY5Y cells (n = 6). (C) Effect of 50 ng/mL growth factor on uninduced SH-SY5Y cells (n = 6). ns, no significance. * $p < 0.05$, ** $p < 0.01$, *** $p < 0.001$, ### $p < 0.001$. 6-OHDA, 6-hydroxydopamine; CQ, chloroquine.

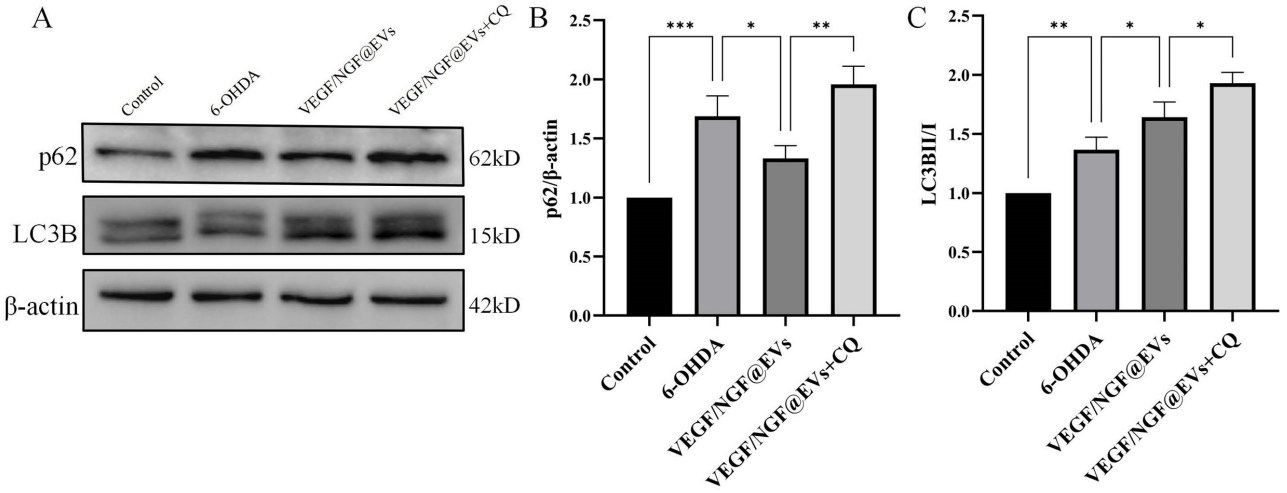

Fig. 4. VEGF/NGF@EVs increased the autophagy of 6-OHDA-induced SH-SY5Y cells (n = 3). (A) Western blotting results. (B) Quantification results of the expressions of p62. (C) Quantification results of the ratio of LC3B-II/I. * $p < 0.05$, ** $p < 0.01$, *** $p < 0.001$. LC3B, microtubule-associated protein 1 light chain 3 beta; p62, sequestosome 1.

with residual neuronal cell bodies exhibiting shrinkage and deformation, a marked decrease in neuronal projections, and lower TH expressions. No significant increase in TH-positive neurons was observed in the blank EVs group, revealing that this EVs dose had no protective effect on dopaminergic neurons. In contrast, both the VEGF@EVs and NGF@EVs groups showed reduced loss of dopaminergic neurons. Neurons in the VEGF@EVs group maintained a relatively intact morphology with many neuronal projections, although some cell bodies demonstrated shrinkage. Neurons in the NGF@EVs group displayed acceptable morphology but fewer neuronal projections. The number of dopaminergic neurons was effectively preserved in the VEGF/NGF@EVs group, with maintained neuronal structure, abundant reticular projections, and a relatively complete cellular architecture.

Subsequently, TH protein expression was measured using WB (Fig. 6B). The results (Fig. 6D) showed that compared with the 6-OHDA group, TH protein levels were significantly higher in the other four experimental groups, with the VEGF/NGF@EVs group showing notably greater effectiveness than the others. Additionally, ELISA results indicated that compared with the model group, striatal DA levels were significantly increased in the VEGF@EVs, NGF@EVs, and VEGF/NGF@EVs groups. Of these, the VEGF/NGF@EVs group showed the most significant in-

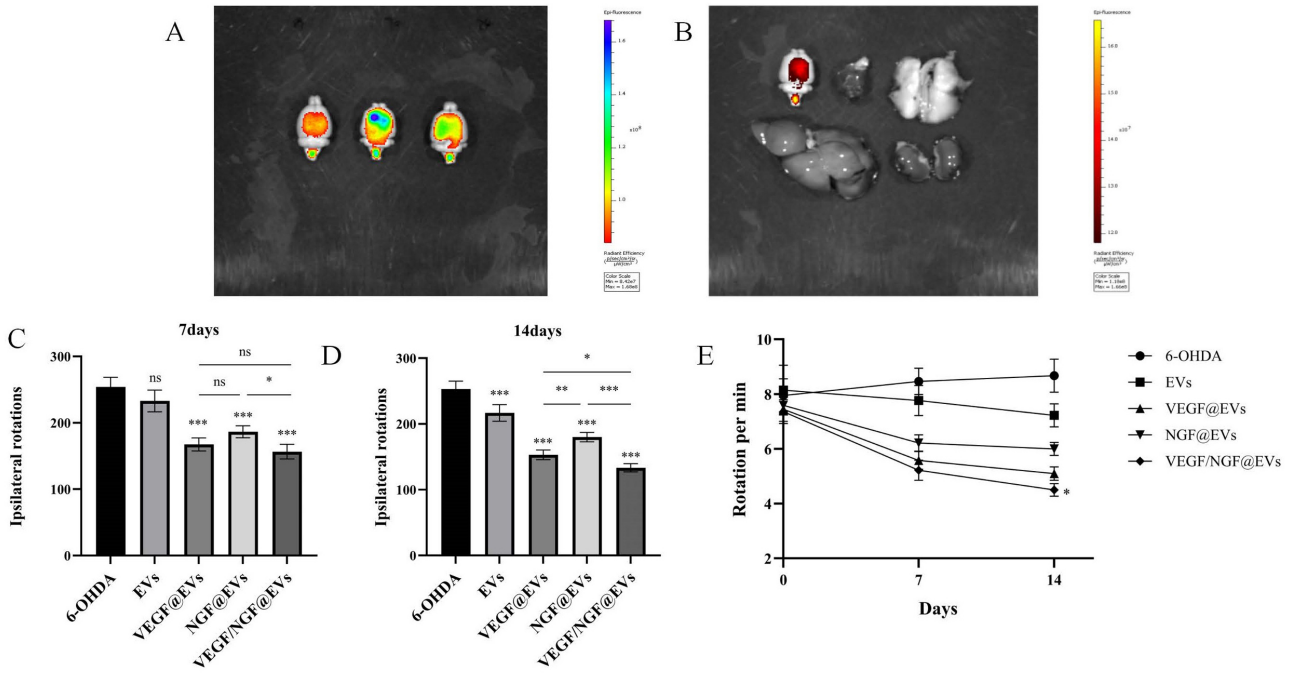

Fig. 5. Accumulation of EVs in the brain of PD rat model and amelioration of behavioral deficits by VEGF/NGF@EVs. (A) Uptake of PKH26-labeled EVs by the brain (n = 3). Left to right: control, 4 h, 16 h. (B) Organ distribution of PKH26-labeled EVs. (C) APO-induced asymmetric rotation after 7 days (n = 8). (D) APO-induced asymmetric rotation after 14 days (n = 8). (E) Changes in APO-induced rotation before and after treatment. * $p < 0.05$, ** $p < 0.01$, *** $p < 0.001$. ns, no significance. PD, Parkinson's disease; APO, apomorphine.

crease in DA levels, markedly higher than those in the single-factor treatment groups (Fig. 6E). These findings suggest that VEGF/NGF@EVs have a strong protective effect on SN dopaminergic neurons.

3.9 The Ability of VEGF/NGF@EVs to Increase Autophagy in the Brains of PD Rats

The WB results (Fig. 7) demonstrated that compared with the control group, the 6-OHDA model group had a lower LC3B-II/I ratio and higher p62 expression, indicating impaired autophagy. After treatment with VEGF@EVs, NGF@EVs, or VEGF/NGF@EVs, the LC3B-II/I ratio increased and p62 levels decreased significantly, suggesting activation of autophagy and recovery of autophagic flux. Of these treatments, the VEGF/NGF@EVs group had the most notable effects, significantly surpassing the single-factor groups, signifying the synergistic effect of VEGF and NGF. These findings align with *in vitro* results, confirming that VEGF/NGF@EVs protect dopaminergic neurons in PD rats by activating autophagy and restoring autophagic flux.

4. Discussion

The irreversible loss of dopaminergic neurons in the midbrain's substantia nigra is a key feature of PD [1]. While its precise cause is not fully understood, critical pathological factors include neurotrophic factor deficiency and impaired autophagy. This study explored the neuroprotective effects of combined VEGF and NGF treatment in PD models and assessed the feasibility of an EV-based codelivery approach. The findings showed that (1) in SH-SY5Y cells, VEGF/NGF@EVs significantly reduced cell death caused by 6-OHDA, with autophagy playing a central role; (2) delivering VEGF and NGF via EVs to the brain markedly improved motor function in PD rats, decreased dopaminergic neuron loss, and mitigated 6-OHDA-induced autophagy suppression.

This study provides clear evidence of the synergistic effects of VEGF and NGF in PD. VEGF and NGF are two growth factors with both angiogenic and neurotrophic properties and have shown beneficial synergistic effects in peripheral nerve regeneration [19,20]. The experiments in this study confirmed the synergistic effects of these two factors in both *in vivo* and *in vitro* settings. Importantly, this study also found that VEGF/NGF@EVs can reverse 6-OHDA-induced inhibition of autophagy, a finding validated both *in vitro* and *in vivo*. This finding links neurotrophic support to the regulation of the intracellular environment, enhancing our understanding of neuroprotective mechanisms.

Existing literature indicates that both VEGF and NGF regulate autophagic processes through the phosphoinositide 3-kinase (PI3K)/protein kinase B (Akt)/mechanistic target of rapamycin (mTOR) signaling pathway [26,27]. Specifically, in the 6-OHDA-induced PD model where autophagic

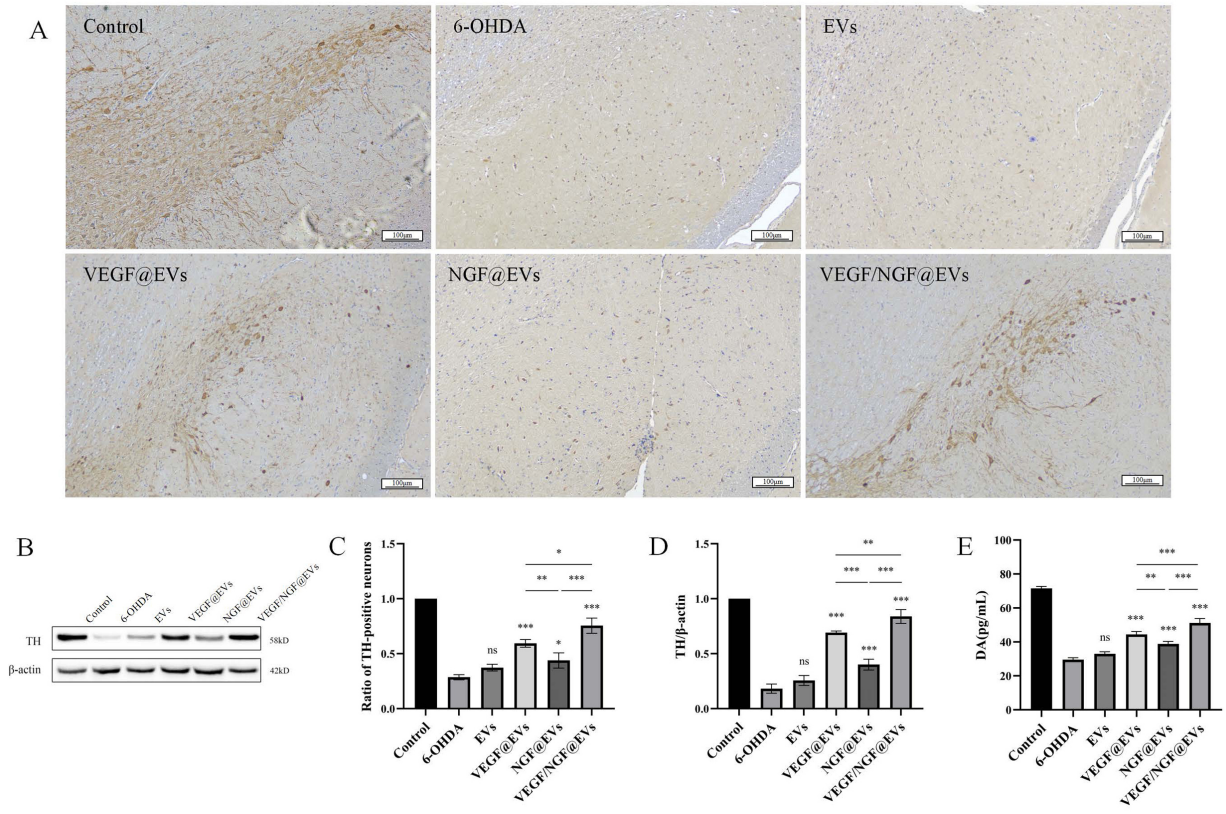

Fig. 6. VEGF/NGF@EVs significantly improved the pathological state in the brain of PD rats (n = 4). (A) IHC results. Scale bar: 100 μm. (B) Western blotting of TH and β-actin. (C) Quantification results of TH-positive dopaminergic neuron counts. (D) Quantification results of the expressions of TH. (E) ELISA assay for DA. * $p < 0.05$, ** $p < 0.01$, *** $p < 0.001$. ns, no significance. IHC, Immunohistochemistry; TH, tyrosine hydroxylase; ELISA, enzyme-linked immunosorbent assay ; DA, dopamine.

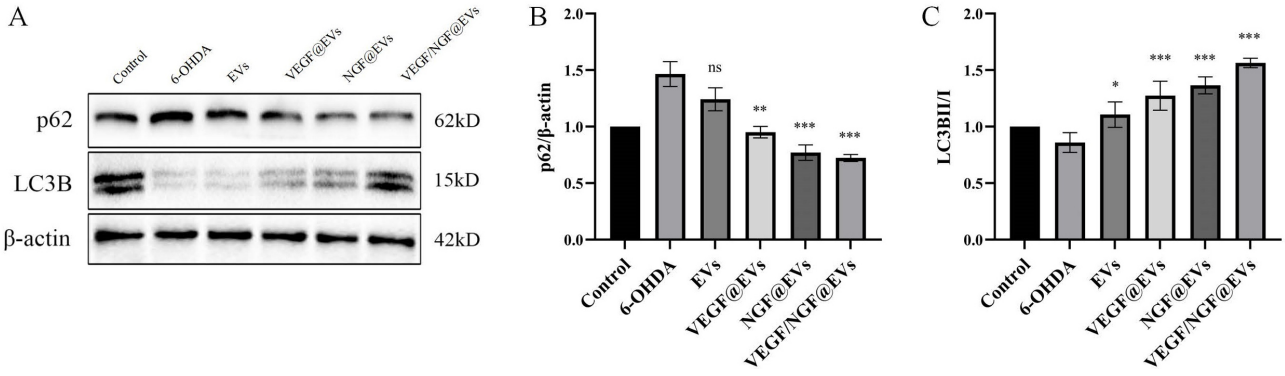

Fig. 7. VEGF/NGF@EVs increased autophagy in the brain of PD rats (n = 4). (A) Western blotting of autophagy proteins. (B) Quantification results of the expressions of p62. (C) Quantification results of the ratio of LC3B-II/I. * $p < 0.05$, ** $p < 0.01$, *** $p < 0.001$. ns, no significance.

flux is typically suppressed, VEGF may relieve this suppression through moderate inhibition of mTOR [28]. Similarly, NGF also enhances autophagy via the PI3K/Akt pathway [29]. Based on these observations, we propose that VEGF and NGF may converge on a shared signaling cascade—the PI3K/Akt/mTOR pathway—to counteract 6-OHDA-induced autophagic inhibition. By simultaneously activating this pathway via EV-mediated codelivery, the two factors may produce a synergistic effect superior to either factor alone, thereby alleviating autophagic arrest and reducing dopaminergic neuron death. This hypothesis is consistent with our experimental finding that combined treatment reversed autophagic suppression.

In addition, a previous study has shown that EVs themselves can modulate autophagic activity in recipient cells [8]. In our cell experiments, pure EVs did not exhibit significant protective effects; however, in animal experiments, repeated administration of EVs alone for 14 days showed a certain degree of autophagic modulation. Based on reports from relevant literature, we speculate that the differential effects of empty EVs between *in vitro* and *in vivo* settings may be attributable to dose accumulation over time [30]. This observation does not diminish the central role of VEGF and NGF.

Another innovation of this study is the use of an EV-mediated codelivery strategy. The large size of proteins and the presence of the BBB have limited drug applications in the central nervous system. Coloading VEGF and NGF into EVs not only ensures their simultaneous delivery and maintains their synergistic ratio but also boosts therapeutic success by harnessing the biological functions of EVs. Cellular uptake experiments confirmed that EV-mediated VEGF/NGF were internalized by 6-OHDA-induced SH-SY5Y cells. Animal experiments clearly demonstrated this strategy's effectiveness: the VEGF/NGF@EVs treatment group showed significantly better survival of dopaminergic neurons and improved rotational behavior. This observation suggests that EVs are a highly promising tool for intracerebral delivery.

This study has significant theoretical and experimental value. Theoretically, it clarifies how VEGF and NGF work together to provide neuroprotection and explores their link to cellular autophagy, offering new support for combination therapies involving neurotrophic factors. In translational medicine, the successful creation and validation of an extracellular vesicle-based dual-protein delivery system introduces new options for intracerebral treatment of PD and other neurological disorders. Compared with viral vectors, synthetic carriers, and repeated intracerebral injections, this approach shows a better safety profile. Through ongoing research and refinement, more effective treatments can be developed for patients with PD to enhance their quality of life.

5. Limitations

Admittedly, this study has certain limitations. First, regarding the growth factor dose ratio, a 1:1 ratio was used in this study, but whether different ratios could yield more significant therapeutic effects remains unknown. Second, although changes in autophagy were observed, the upstream signaling pathways, such as PI3K/Akt/mTOR, that regulate autophagy have not been fully elucidated and require further investigation. Lastly, while the efficacy was confirmed in the acute 6-OHDA model, PD is a chronic progressive disorder. Future research should assess the therapeutic effects of this approach in delaying disease progression and examine the long-term safety of prolonged treatment.

6. Conclusions

This study systematically explored the neuroprotective mechanisms and therapeutic potential of VEGF/NGF@EVs therapy using both *in vitro* and *in vivo* experiments. Cellular studies showed that VEGF/NGF@EVs significantly increase the viability of SH-SY5Y cell models and reverse 6-OHDA-induced inhibition of autophagy. In animal trials, VEGF/NGF@EVs effectively achieve brain-targeted delivery in PD rats, greatly protecting dopaminergic neurons in the substantia nigra and enhancing motor function. This work provides new mechanistic insights into combination therapy for 6-OHDA-induced PD models and offers fresh perspectives for targeted delivery in central nervous system disorders.

Abbreviations

PD, Parkinson's disease; EVs, extracellular vesicles; VEGF, vascular endothelial growth factor; NGF, nerve growth factor; 6-OHDA, 6-Hydroxydopamine hydrochloride; HUC-MSCs, human umbilical cord mesenchymal stem cells; TEM, transmission electron microscopy; NTA, nanoparticle tracking analysis; BBB, blood–brain barrier; CQ, chloroquine; TH, tyrosine hydroxylase; DA, dopamine.

Availability of Data and Materials

All data reported in this paper will also be shared by the lead contact upon request.

Author Contributions

XL designed the research study. WY performed the research and wrote the manuscript. FH, XM, YW and CW were involved in the study design, data acquisition, and analysis and interpretation. . All authors contributed to editorial changes in the manuscript. All authors read and approved the final manuscript. All authors have participated sufficiently in the work and agreed to be accountable for all aspects of the work.

Ethics Approval and Consent to Participate

The research protocol was approved by the Ethics Committee of Liaocheng People's Hospital (Ethic Approval Number: 2022085). All experimental procedures were approved by the Animal Care and Use Committee of Shandong First Medical University and conducted in accordance with the Chinese Council on Animal Care guidelines and the ARRIVE 2.0 guidelines (**Supplementary Material**).

Acknowledgment

We gratefully acknowledge the assistance and instruction from Professor Nan Zhang of Key Laboratory for Stem Cell & Regenerative Medicine Translation of Health Commission of Shandong Province Liaocheng Hospital Affiliated to Shandong First Medical University.

Funding

This research received no external funding.

Conflicts of Interest

The authors declare no conflicts of interest.

Supplementary Material

Supplementary material associated with this article can be found, in the online version, at https://doi.org/10.31083/JIN50932.

References

[1] Morris HR, Spillantini MG, Sue CM, Williams-Gray CH. The pathogenesis of Parkinson's disease. Lancet (London, England). 2024; 403: 293–304. https://doi.org/10.1016/S0140-6736(23)01478-2

[2] Zhou ZD, Yi LX, Wang DQ, Lim TM, Tan EK. Role of dopamine in the pathophysiology of Parkinson's disease. Translational Neurodegeneration. 2023; 12: 44. https://doi.org/10.1186/s40035-023-00378-6

[3] Foltynie T, Bruno V, Fox S, Kühn AA, Lindop F, Lees AJ. Medical, surgical, and physical treatments for Parkinson's disease. Lancet (London, England). 2024; 403: 305–324. https://doi.org/10.1016/S0140-6736(23)01429-0

[4] Mizushima N, Komatsu M. Autophagy: renovation of cells and tissues. Cell. 2011; 147: 728–741. https://doi.org/10.1016/j.cell.2011.10.026

[5] Sarkar S. Regulation of autophagy by mTOR-dependent and mTOR-independent pathways: autophagy dysfunction in neurodegenerative diseases and therapeutic application of autophagy enhancers. Biochemical Society Transactions. 2013; 41: 1103–1130. https://doi.org/10.1042/BST20130134

[6] Tu HY, Yuan BS, Hou XO, Zhang XJ, Pei CS, Ma YT, et al. α-synuclein suppresses microglial autophagy and promotes neurodegeneration in a mouse model of Parkinson's disease. Aging Cell. 2021; 20: e13522. https://doi.org/10.1111/acel.13522

[7] He HJ, Xiong X, Zhou S, Zhang XR, Zhao X, Chen L, et al. Neuroprotective effects of curcumin via autophagy induction in 6-hydroxydopamine Parkinson's models. Neurochemistry International. 2022; 155: 105297. https://doi.org/10.1016/j.neuint.2022.105297

[8] Chen HX, Liang FC, Gu P, Xu BL, Xu HJ, Wang WT, et al. Exosomes derived from mesenchymal stem cells repair a Parkinson's disease model by inducing autophagy. Cell Death & Disease. 2020; 11: 288. https://doi.org/10.1038/s41419-020-2473-5

[9] Sul JH, Shin S, Kim HK, Han J, Kim J, Son S, et al. Dopamine-conjugated extracellular vesicles induce autophagy in Parkinson's disease. Journal of Extracellular Vesicles. 2024; 13: e70018. https://doi.org/10.1002/jev2.70018 Erratum in: Journal of Extracellular Vesicles. 2025; 14: e70082. https://doi.org/10.1002/jev2.70082

[10] Yasuhara T, Shingo T, Muraoka K, Kameda M, Agari T, Wen Ji Y, et al. Neurorescue effects of VEGF on a rat model of Parkinson's disease. Brain Research. 2005; 1053: 10–18. https://doi.org/10.1016/j.brainres.2005.05.027

[11] Sheikh MA, Malik YS, Xing Z, Guo Z, Tian H, Zhu X, et al. Polylysine-modified polyethylenimine (PEI-PLL) mediated VEGF gene delivery protects dopaminergic neurons in cell culture and in rat models of Parkinson's Disease (PD). Acta Biomaterialia. 2017; 54: 58–68. https://doi.org/10.1016/j.actbio.2016.12.048

[12] Meng XY, Huang AQ, Khan A, Zhang L, Sun XQ, Song H, et al. Vascular endothelial growth factor-loaded poly-lactic-co-glycolic acid nanoparticles with controlled release protect the dopaminergic neurons in Parkinson's rats. Chemical Biology & Drug Design. 2020; 95: 631–639. https://doi.org/10.1111/cbdd.13681

[13] Zou J, Chen Z, Wei X, Chen Z, Fu Y, Yang X, et al. Cystatin C as a potential therapeutic mediator against Parkinson's disease via VEGF-induced angiogenesis and enhanced neuronal autophagy in neurovascular units. Cell Death & Disease. 2017; 8: e2854. https://doi.org/10.1038/cddis.2017.240

[14] Norata D, Capone F, Motolese F, Marano M, Rossi M, Calandrelli R, et al. 1953-2023. Seventy Years of the Nerve Growth Factor: A Potential Novel Treatment in Neurological Diseases? Aging and Disease. 2024; 16: 2293–2314. https://doi.org/10.14336/AD.2024.0573

[15] Yang C, Zhao J, Cheng Y, Le XC, Rong J. N-Propargyl Caffeate Amide (PACA) Potentiates Nerve Growth Factor (NGF)-Induced Neurite Outgrowth and Attenuates 6-Hydroxydopamine (6-OHDA)-Induced Toxicity by Activating the Nrf2/HO-1 Pathway. ACS Chemical Neuroscience. 2015; 6: 1560–1569. https://doi.org/10.1021/acschemneuro.5b00115

[16] Luo D, Zhao J, Cheng Y, Lee SMY, Rong J. N-Propargyl Caffeamide (PACA) Ameliorates Dopaminergic Neuronal Loss and Motor Dysfunctions in MPTP Mouse Model of Parkinson's Disease and in MPP^+-Induced Neurons via Promoting the Conversion of proNGF to NGF. Molecular Neurobiology. 2018; 55: 2258–2267. https://doi.org/10.1007/s12035-017-0486-6

[17] Lorigados Pedre L, Pavón Fuentes N, Alvarez González L, McRae A, Serrano Sánchez T, Blanco Lescano L, et al. Nerve growth factor levels in Parkinson disease and experimental parkinsonian rats. Brain Research. 2002; 952: 122–127. https://doi.org/10.1016/s0006-8993(02)03222-5

[18] Shimoke K, Chiba H. Nerve growth factor prevents 1-methyl-4-phenyl-1,2,3,6-tetrahydropyridine-induced cell death via the Akt pathway by suppressing caspase-3-like activity using PC12 cells: relevance to therapeutical application for Parkinson's disease. Journal of Neuroscience Research. 2001; 63: 402–409. https://doi.org/10.1002/1097-4547(20010301)63:5<402::AID-JNR1035>3.0.CO;2-F

[19] Calza L, Giardino L, Giuliani A, Aloe L, Levi-Montalcini R. Nerve growth factor control of neuronal expression of angiogenetic and vasoactive factors. Proceedings of the National Academy of Sciences of the United States of America. 2001; 98: 4160–4165. https://doi.org/10.1073/pnas.051626998

[20] Xia B, Lv Y. Dual-delivery of VEGF and NGF by emulsion electrospun nanofibrous scaffold for peripheral nerve regeneration. Materials Science & Engineering. C, Materials for Biological Applications. 2018; 82: 253–264. https://doi.org/10.1016/j.msec.2017.08.030

[21] Liu S, Liu Y, Zhou L, Li C, Zhang M, Zhang F, et al. XT-type DNA hydrogels loaded with VEGF and NGF promote peripheral nerve regeneration *via* a biphasic release profile. Biomaterials Science. 2021; 9: 8221–8234. https://doi.org/10.1039/d1bm01377g

[22] Welsh JA, Goberdhan DCI, O'Driscoll L, Buzas EI, Blenkiron C, Bussolati B, et al. Minimal information for studies of extracellular vesicles (MISEV2023): From basic to advanced approaches. Journal of Extracellular Vesicles. 2024; 13: e12404. https://doi.org/10.1002/jev2.12404 Erratum in: Journal of Extracellular Vesicles. 2024; 13: e12451. https://doi.org/10.1002/jev2.12451

[23] Chen P, Wang F, Ling B, Zhu Y, Lin H, Huang J, et al. Mesenchymal Stem Cell-Derived Extracellular Vesicles: Emerging Therapies for Neurodegenerative Diseases. International Journal of Nanomedicine. 2025; 20: 8547–8565. https://doi.org/10.2147/IJN.S526945

[24] Wang CC, Hu XM, Long YF, Huang HR, He Y, Xu ZR, et al. Treatment of Parkinson's disease model with human umbilical cord mesenchymal stem cell-derived exosomes loaded with BDNF. Life Sciences. 2024; 356: 123014. https://doi.org/10.1016/j.lfs.2024.123014

[25] Shie MY, Chen MC, Chen Y, Huang SW, Lin YH, Yu MH, et al. Engineered extracellular vesicles-mediated curcumin delivery in brain microenvironment modulating lysosomes, mitochondria, and microglia reprogram for parkinson's disease therapy. Journal of Nanobiotechnology. 2025; 24: 46. https://doi.org/10.1186/s12951-025-03911-z

[26] Kang K, Wang DP, Lv QL, Chen F. VEGF-A ameliorates ischemia hippocampal neural injury via regulating autophagy and Akt/CREB signaling in a rat model of chronic cerebral hypoperfusion. Journal of Stroke and Cerebrovascular Diseases : the Official Journal of National Stroke Association. 2023; 32: 107367. https://doi.org/10.1016/j.jstrokecerebrovasdis.2023.107367

[27] Li R, Li D, Wu C, Ye L, Wu Y, Yuan Y, et al. Nerve growth factor activates autophagy in Schwann cells to enhance myelin debris clearance and to expedite nerve regeneration. Theranostics. 2020; 10: 1649–1677. https://doi.org/10.7150/thno.40919

[28] Chen L, Lin G, Chen K, Wan F, Liang R, Sun Y, et al. VEGF knockdown enhances radiosensitivity of nasopharyngeal carcinoma by inhibiting autophagy through the activation of mTOR pathway. Scientific Reports. 2020; 10: 16328. https://doi.org/10.1038/s41598-020-73310-x

[29] Li Y, Wu F, Zhou M, Zhou J, Cui S, Guo J, et al. ProNGF/NGF Modulates Autophagy and Apoptosis through PI3K/Akt/mTOR and ERK Signaling Pathways following Cerebral Ischemia-Reperfusion in Rats. Oxidative Medicine and Cellular Longevity. 2022; 2022: 6098191. https://doi.org/10.1155/2022/6098191

[30] Hagey DW, Ojansivu M, Bostancioglu BR, Saher O, Bost JP, Gustafsson MO, et al. The cellular response to extracellular vesicles is dependent on their cell source and dose. Science Advances. 2023; 9: eadh1168. https://doi.org/10.1126/sciadv.adh1168